International Journal on Magnetic Particle Imaging
Vol 8, No 1, Suppl 1, Article ID 2203040, 4 Pages

Infinite Science Publishing

Proceedings Article

Enhanced characterization of a magnetic particle imaging tracer combining field-flow fractionation and magnetic particle spectroscopy

A. Remmo[a,*] · N. Löwa[a] · J. Peter[b] · F. Wiekhorst[a]

[a]Physikalisch-Technische Bundesanstalt (Metrology for Magnetic Nanoparticles), Abbestr. 2-12, 10587 Berlin, GER
[b]Technische Universität Berlin (Institut für Strömungsmechanik und Technische Akustik), Straße des 17.Juni 135, 10623 Berlin, GER
*Corresponding author, email: amani.remmo@ptb.de

Abstract

For a more detailed assessment of the performance of magnetic nanoparticles used as tracer in magnetic particle imaging, we applied centrifugal flow-field fractionation (CF3) to separate a tracer according to their density and mass. The fractions were then magnetically and physically characterized by MPS, DLS, MALS and UV/Vis. Combining these findings with the results of magnetic characterization will allow a better understanding of the underlying mechanisms of MPI signal generation and tracer performance.

I. Introduction

Magnetic particle imaging (MPI) is an imaging modality that utilizes magnetic iron oxide nanoparticles as tracers with great promise for clinical application in angiography, hyperthermia, and oncology [1]. Its exceptional contrast, high sensitivity, and good spatial resolution highly depends on the magnetic properties of the magnetic nanoparticles (MNP) used as tracers and thus, ongoing optimization of MNP is carried out to further improve their imaging performance [2]. The magnetic properties of MNP strongly depend on their size distribution [2] [3] and many MNP systems exhibit a rather broad size distribution so that only a small fraction of particles has the dominating contribution to the MPI signal [4]. For a long time, the clinically tested MRI liver contrast agent Resovist® has been used as an MPI tracer with excellent performance. Studies have shown that Resovist® has a bimodal size distribution consisting of a small fraction with (mean) particle diameters of about 5 nm and larger fraction of about 24 nm [5]. The latter fraction is attributed to be responsible for the high MPI performance [6] [7]. Therefore, the decomposition of a MNP distribution into smaller fractions and the determination of the corresponding MPI performance is of great interest for tracer optimization of other MNP systems. Field-flow fractionation (F3) techniques are powerful tools for separating the distribution of an MNP system with respect to a specific property. All F3 techniques are based on the same operating principle. A laminar flow carries the analyte through a flat channel in which different flow velocities result from the parabolic flow profile. Due to a vertical separation field (e.g., fields as a consequence of a fluid flow, centrifugation, temperature gradient, or grav-

10.18416/ijmpi.2022.2203040

ity) and the counteracting diffusion, particles with different properties have different velocities in the channel [8]. As a result, an MNP distribution injected into the F3 will leave the separation channel sorted with respect to a particular property (e.g., size, mass) [9]. F3 techniques become a powerful analytical tool by combining them with different detectors to determine physical properties such as hydrodynamic diameter, iron mass, or core diameter during the fractionation. In this work, we combined centrifugal field-flow fractionation (CF3) with magnetic particle spectroscopy (MPS) as a magnetic detector to determine the MPI performance of MNP fractions. Ultraviolet and visible spectroscopy (UV/Vis) is used to determine the concentration of the isolated fractions. The size distribution is analyzed by using the Dynamic light scattering (DLS) and multi-angle light scattering (MALS). In this way, the CF3 combined with a multidetector array forms a platform for thorough magnetic and structural characterization of MNP systems and detailed evaluation of MPI tracer performance.

II. Material and methods

This chapter discusses the experimental methods that have been used in this work.

II.I. Magnetic nanoparticles and Media

Two MNP systems, Resovist® (RV, *Bayer HealthCare*) and SHP 25-50 (S25, *Ocean Nanotech*) were selected for this study. RV is an aqueous suspension of iron oxide particles coated with carboxydextran. Since RV contains two particle populations (single and multicore MNP), it is ideally suited for multi-detector F3 analysis [5]. In contrast to RV, S25 is composed of monodisperse single core MNP, only. Details of origin, coating, and physical parameters of the MNP systems are summarized in Tab. 1. All chemicals used in this study were of analytical reagent grade. Deionized water (ddH_2O) containing FL-70 detergent (Fisher Sci., USA) and sodium chloride (NaCl, Merck, GER) was used as carrier liquid for fractionation.

II.II. CF3

Mass sensitive separation of MNP was performed using a commercial CF3 system (*Postnova Analytics GmbH, GER*). The CF3 is one of the F3 techniques that has been used for separation of particles in the range of 10 nm to 20 µm [10]. The separation mechanism of CF3 is described in detail in [8][10]. Briefly, in CF3 the particles are forced against the accumulation wall by a vertically acting centrifugal forces (see Fig. 1). The parabolic flow in the flat channel finally leads to a temporal separation of the particles of different mass.

Due to the effect of diffusion, the concentration $c(x)$ of the particles decreases exponentially with the distance x from the accumulation wall of the channel: $c(x) = c_0 e^{-x/l}$, where c_0 is the analyte concentration at the accumulation wall ($x = 0$) and l is the center-of-gravity distance from the accumulation wall at equilibrium [11].

The parameter l can be expressed by the dimensionless retention parameter $\lambda = l/w$, where w is the channel thickness. For CF3, λ can be expressed as: $\lambda = 6kT/(\pi|\rho_p - \rho|wgd^3)$, where $T = 293$ K is the temperature of the medium, k is the Boltzmann constant ($1.38 \cdot 10^{-23}$ kg m^2 s^{-2} K^{-1}), $\rho_p = 5200$ kg/m^3 is the particle density, $\rho = 997$ kg/m^3 is the solvent density, r is the rotor radius, ω is the angular rotation frequency, and d is the equivalent spherical MNP diameter. The retention parameter λ represents the link between theoretical and measurable experimental parameters through the retention ratio R, which is defined as the ratio of void time t_0 and analyte retention time t_r. R is related to λ by [11]:

$$R = \frac{t_0}{t_r} = 6\lambda \coth\left(\frac{1}{2\lambda}\right) - 12\lambda^2 . \quad (1)$$

The optimal range for R is approximately $0.03 \leq R \leq 0.2$ [11]. In this study a rotation speed of $\nu_{rot} = 4900$ 1/min, ddH_2O as carrier liquid and a particle concentration of c(Fe)=10 mmol/L is used to achieve low sample loss, avoid channel overloading effects, and enable high-resolution separation ($R = 0.03$).

II.III. Detectors

The detector array consisted of a UV/Vis detector for concentration determination, a MALS detector (both *Postnova Analytics GmbH*), and a DLS detector (Zetasizer NanoZS, *Malvern*) for size determination, and a magnetic particle spectrometer (MPS-3, *Bruker BioSpin*) for magnetic characterization. Angular dependent scattering profiles of MALS were used to obtain the root-mean-square radius, commonly named radius of gyration r_g. The core diameter d_C of an equivalent sphere was calculated by the following equation: $d_c = \sqrt{20/3} \cdot r_g$ [12]. The hydrodynamic size d_{hyd} was determined by DLS measuring the fluctuations of the scattered light at an angle of 173° to determine the diffusion coefficient D, which is inversely proportional to d_{hyd}. In MPS, a sinusoidal excitation field of B=25 mT amplitude at a frequency f_0=25 kHz is applied to an MNP sample. Due to the non-linear magnetization of the MNP, the measured response contains distinct odd multiples of f_0 (i.e. higher harmonics A_i). The third harmonic amplitude A_3 is directly proportional to the absolute MNP content and can be used for MNP quantification. To compare different MNP systems, the specific amplitude A_3* is calculated; that is the A_3 amplitude normalized to the absolute iron mass of the sample. The shape of the spectrum is characterized by concentration independent ratio A_5/A_3 as a fingerprint of the dynamic magnetic behavior of MNP.

10.18416/ijmpi.2022.2203040

Table 1: Sample name, ID (used within the work), supplier and the coating of the MNP. Furthermore, the hydrodynamic diameter dhyd (z-average) and polydispersity index (PDI) obtained by DLS and characteristic MPS parameters A_3* normalized to iron amount and amplitude ratio A_5/A_3 as determined at 25 mT, f_0=25 kHz for the stock suspension are presented. The numbers in parentheses denote the uncertainty of the last digit, e.g. 58.3(1) reads as 58.3±0.3 nm.

sample	ID	supplier	coating	d_{hyd} / (nm)	PDI	A_3* / (Am^2/kg(Fe))	A_5/A_3 / (%)
Resovist	RV	Bayer Healthcare	carboxy dextran	58.3(1)	0.29(5)	8.67(3)	41.31(1)
SHP 25-50	S25	Ocean Nanotech	carboxylic acid	58(2)	0.13(6)	20.62(3)	41.56(1)

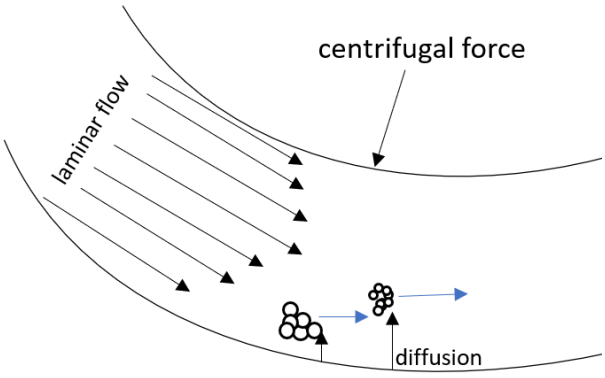

Figure 1: Working principle of centrifugal field-flow fractionation.

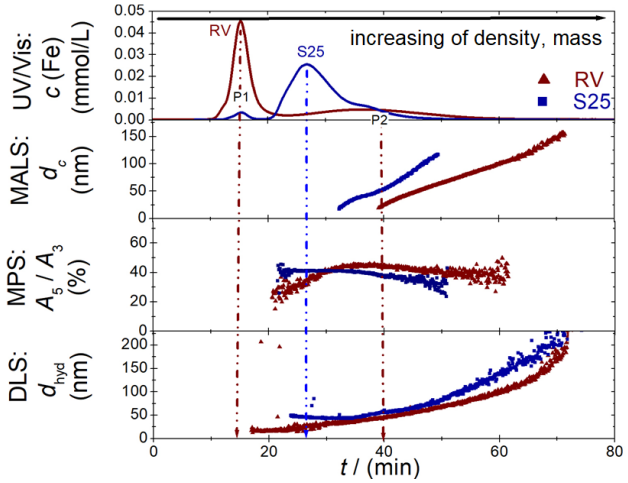

Figure 2: UV/Vis (a), MALS (b), MPS (c), and DLS (d) elugrams during CF3 of RV (red) and S25 (blue). After CF3, the separation of the two particle populations (P1-small particles, P2-large particles) in RV is clearly visible in UV/Vis. The other detectors show rather broad distributions of properties (size) in RV as well as S25.

III. Results and discussion

The separation by CF3 clearly resolves the two different particle populations of RV confirming previous studies [2], [13] (see Fig. 2a). In addition, the MPS reveals the different magnetic behavior of the two RV populations and enables a targeted optimization of MPI tracers like RV. The size determination (Fig.2 b, d) resulted in d_{hyd}=22 nm for the small particle population of RV and d_c=21 nm and d_{hyd}=46 nm for the large particle population of RV which agrees with previous fractionations of RV using AF4 [13][14]. Since size determination by MALS is only possible for diameter above $d_c \approx 20$ nm, the smaller population of RV could not be resolved. The magnetic moments of RV in the larger population is about $A_5/A_3 = 45\%$ (Fig. 2c, $t = 40$ min) measured by MPS. In contrast to RV, the UV/Vis-elugram of S25 reveals that this MNP-system consists of one population, only. Furthermore, a d_{hyd} of 45 nm was determined by DLS with a corresponding A_5/A_3 of 41 % measured by MPS (Fig. 2c, t= 27 min). For both MNP systems (RV, S25), the iron concentrations of the resulting fractions are very low (<50 µmol/L). Compared to AF4 which uses a stream splitter five times higher concentration could be achieved [13]. Nevertheless, the fractions of the analytical F3 separations without post-processing (e.g. concentration) are initially not suitable for further studies with MPI.

IV. Conclusions

In this work, we have demonstrated the potential of a multidetector CF3 system to evaluate the MPI performance of MNP systems. Therefore, we used a combination of magnetic (MPS) and structural (UV/Vis, MALS, and DLS) detectors to characterize MNP systems which were separated to their density and mass. This multidetector platform enables accurate determination of magnetic properties and size of MNP in a single step, regardless of the presence of a monomodal or multimodal size distribution, making it superior to conventional characterization techniques.

Acknowledgments

Research funding: This project was partially funded by the Deutsche Forschungsgemeinschaft (DFG, German Research Foundation) within the research grant “CellMPI” (455706279).

Author's statement

Conflict of interest: Authors state no conflict of interest. Informed consent: Informed consent has been obtained from all individuals included in this study. Ethical approval: The research related to human use complies with all the relevant national regulations, institutional policies and was performed in accordance with the tenets of the Helsinki Declaration, and has been approved by the authors' institutional review board or equivalent committee.

References

[1] E. Y. Yu u. a., „Magnetic Particle Imaging: A Novel in Vivo Imaging Platform for Cancer Detection", Nano Lett., Bd. 17, Nr. 3, S. 1648–1654, März 2017, doi: 10.1021/acs.nanolett.6b04865.

[2] D. Eberbeck, F. Wiekhorst, S. Wagner, und L. Trahms, „How the size distribution of magnetic nanoparticles determines their magnetic particle imaging performance", Appl. Phys. Lett., Bd. 98, Nr. 18, S. 182502, Mai 2011, doi: 10.1063/1.3586776.

[3] F. Ludwig u. a., „Optimization of Magnetic Nanoparticles for Magnetic Particle Imaging", IEEE Trans. Magn., Bd. 48, Nr. 11, S. 3780–3783, Nov. 2012, doi: 10.1109/TMAG.2012.2197601.

[4] N. Löwa, D. Eberbeck, U. Steinhoff, F. Wiekhorst, und L. Trahms, „Potential of Improving MPI Performance by Magnetic Separation", in Magnetic Particle Imaging, Bd. 140, T. M. Buzug und J. Borgert, Hrsg. Berlin, Heidelberg: Springer Berlin Heidelberg, 2012, S. 73–78. doi: 10.1007/978-3-642-24133-8_12.

[5] A. F. Thünemann, S. Rolf, P. Knappe, und S. Weidner, „In Situ Analysis of a Bimodal Size Distribution of Superparamagnetic Nanoparticles", Anal. Chem., Bd. 81, Nr. 1, S. 296-301, Jan. 2009, doi: 10.1021/ac802009q.

[6] P. Pasmans, „Magnetic nanoparticles for Magnetic Particle Imaging: from particle characterization to image simulations", student thesis, 2009.

[7] D. Eberbeck, C. L. Dennis, N. F. Huls, K. L. Krycka, C. Gruttner, und F. Westphal, „Multicore Magnetic Nanoparticles for Magnetic Particle Imaging", IEEE Trans. Magn., Bd. 49, Nr. 1, S. 269–274, Jan. 2013, doi: 10.1109/TMAG.2012.2226438.

[8] J. Janca und J. Chmelik, „Focusing in field-flow fractionation", Anal. Chem., Bd. 56, Nr. 13, S. 2481–2484, Nov. 1984, doi: 10.1021/ac00277a049.

[9] J. C. Giddings, „Field-Flow Fractionation: Analysis of Macromolecular, Colloidal, and Particulate Materials", Science, Bd. 260, Nr. 5113, S. 1456–1465, Juni 1993, doi: 10.1126/science.8502990.

[10] F. J. F. Yang, M. N. Myers, und J. Calvin. Giddings, „Programmed sedimentation field-flow fractionation", Anal. Chem., Bd. 46, Nr. 13, S. 1924–1930, Nov. 1974, doi: 10.1021/ac60349a009.

[11] J. Gigault, J. M. Pettibone, C. Schmitt, und V. A. Hackley, „Rational strategy for characterization of nanoscale particles by asymmetric-flow field flow fractionation: A tutorial", Analytica Chimica Acta, Bd. 809, S. 9–24, Jan. 2014, doi: 10.1016/j.aca.2013.11.021.

[12] F. R. Schwarzl, Polymermechanik: Struktur und mechanisches Verhalten von Polymeren. Berlin: Springer-Verlag, 2011.

[13] N. Löwa, P. Radon, D. Gutkelch, R. August, und F. Wiekhorst, „Hyphenation of Field-Flow Fractionation and Magnetic Particle Spectroscopy", Chromatography, Bd. 2, Nr. 4, S. 655–668, Nov. 2015, doi: 10.3390/chromatography2040655.

[14] N. Löwa, „Messung und Analyse magnetischer Nanopartikel Untersuchung des Zusammenhangs zwischen dem NMR-Verhalten und der Struktur sowie den magnetischen Eigenschaften verschiedener superparamagnetischer Eisenoxid-Nanopartikel", Diplomarbeit, Technische Universität Berlin, Berlin, 2011.

